Journal of Computer-Aided Molecular Design, 6 (1992) 79–91
ESCOM

J-CAMD 142

Computer simulation of the conformational behaviour of angiotensinogen (6-13) renin substrate

M. Benkoulouche[a], M. Cotrait[a,*] and B. Maigret[b]

[a]*Laboratoire de Cristallographie, URA 144 du CNRS, 351 cours de la Libération, F-33405 Talence Cedex, France*
[b]*Laboratoire de RMN et de Modélisation Moléculaire, UMR 50 du CNRS, Institut LeBel, Université Louis Pasteur, 4 rue Blaise Pascal, F-67000 Strasbourg, France*

Received 2 January 1991
Accepted 24 July 1991

Key words: Angiotensinogen (6-13); Monte-Carlo methods; Cluster analysis; Conformational analysis

SUMMARY

The conformational behaviour of the biologically active angiotensinogen (6-13) fragment has been investigated by computer simulations. A large sample of conformers has been generated using the Monte-Carlo procedure, then analysed using classification and partition methods. Seven families can describe the conformational distribution. About 40% of conformers are fully extended, 28% are folded at the C-terminal His^6-Pro^7-Phe^8-His^9 level and the others are folded at different levels. The study highlights the extreme flexibility of the angiotensinogen fragment.

INTRODUCTION

The renin-angiotensin system is essential for normal blood pressure regulation. The first step of this biological cascade requires cleavage of the protein angiotensinogen by the highly specific enzyme renin. The only peptide bonds that have been found to be hydrolysed by renin are the Leu^9-Leu^{10} bond in the equine substrate [1] and the Leu-Val bond in the human substrate [2]. The minimum sequence showing a good affinity for the equine renin protease has been found to be the octa-peptide His-Pro-Phe-His-Leu-Leu-Val-Tyr: angiotensinogen (6-13) [1].

Many conformational studies on angiotensin I and particularly on angiotensin II have been reported, using NMR, Raman spectroscopy, fluorescence and theoretical conformational analysis [3–7]. Unfortunately, much less has been reported on the structure of intermediate angiotensino-

* To whom correspondence should be addressed.

gen fragments including the Leu^{10}-Leu^{11} bond, hydrolyzed by renin to give angiotensin I. A study by Nakaie et al. [8] proposed a model characterized by a β-turn involving the His^6 and His^9 residues; moreover, they showed that conformationally restricted analogues, such as [Cys^5, Cys^{10}] angiotensinogen (5-14), where the β-turn structure is stabilized by an S-S cystine bond, are competitive inhibitors of renin.

In the last few years we have investigated the conformation of equine angiotensinogen (6-13) and some of its fragments. The crystal structures of Ac-Pro-Phe-His [9], Leu-Leu-Val-Tyr-OMe [10] and φ-O-CH_2O-Leu-Val-Phe-O-Me [11] and the conformational analysis of Ac-His-Pro-Phe-His-MA using molecular mechanics [9] have recently been reported.

The availability of crystal samples of equine angiotensinogen fragments suitable for X-ray diffraction analysis has prompted theoretical investigations in order to compare their conformational preferences with those of the crystal. Moreover, as mentioned above, there is little information on the conformational aspects of angiotensinogen fragments, in either their human or equine form.

We present a conformational analysis of angiotensinogen (6-13) using Monte-Carlo methods due to the great number of conformations accessible to such a long linear peptide.

METHODS

Generation and description of conformers

A large sample of conformers may be generated by the Monte-Carlo technique using the Metropolis algorithm [12]. This procedure has been used for conformational simulations and has proved to be an efficient way to explore an energy hyper-surface [13, 14]. Whereas efficient strategies have been designed to circumvent the multiple-minima problem in peptides [15], the latter's inherent flexibility often warrants an exhaustive sampling of all families of conformers, prone to coexist within a limited energetic boundary and in a given environment. One means toward this end consists in the use of Monte-Carlo techniques, coupled to a cluster analysis [16, 17].

This procedure can be used in unraveling the conformational characteristics of small peptides. A particularly significant example is that of enkephalin [18]. It was shown that despite the very large number of accessible values in the space of torsional angles for this molecule, its conformational patterns could be regrouped in separate clusters, within each of which, well-defined, closely comparable intramolecular interatomic distances could be found in common. This technique is used in the present investigation.

The Monte-Carlo (Metropolis) procedure works as follows: a starting conformation **i** is initialized for the considered peptide by picking randomly selected (φ, ψ) dihedral angles in the Ramachandran energy map of each individual residue in the sequence; the energy for this conformer, E_i, is calculated. This conformer is then randomly modified by selecting a new (φ, ψ) couple in the Ramachandran map of a randomly selected residue, where φ and ψ angles intervals between neighbouring points are only 15°. The χi angles were allowed to change by 30° steps*.

*It should be remembered that in peptides and proteins the angle is preferentially close to 180° and 300° [19].

The energy of the $\mathbf{j}^{th}$ conformer E_j is then calculated:

– if $E_j < E_i$, then conformation **j** is considered as the new conformational state and the process is repeated.

– if $E_j > E_i$, then conformation **j** is nevertheless retained according to its Boltzmann factor p_j and to the transition probability p_j/p_i used in the well-known Metropolis test [12].

The number, N_2, of iterations depends on the point where the final energy becomes more or less stable.

The whole procedure was run from N_1 different starting conformers in order to effectively sample the conformational distribution. This Markovian random walk through the conformational space should prevent the molecule from being trapped in one of the numerous local energy minima of the conformational hypersurface [20].

In the present calculations, 50 starting conformers were randomly selected, and each was improved during 2000 steps, so that 100000 conformers were thus generated. From these 100000 conformations, 2735 different stable conformers were retained as 'new states' and used to sample the peptide energy space.

The retention of 2735 conformers out of 100000 generated was guided by an energy criterion, rejecting all conformers that had a relative conformational energy greater than 10 kcal/mol above that of the most stable conformer of the sample. The minimum energy $(E_{min})^*$ and the average energy $(E_{moy})^*$ for each cluster were added to the Table 3. The runs were performed at 300 K.

The conformational energy terms were computed using a molecular mechanics approach with the force field of Scheraga [21]. In the crystal structures of angiotensinogen fragments, the histidyl residue is always protonated [9]. We thus decided to consider histidines in their protonated state, as is the case at the pH of the biological medium (pH 5–7). A value of 8 was selected for the dielectric constant ε, as justified in previous studies [22, 23].

In keeping with our previous theoretical investigation on charged oligopeptides [22, 23], the N- and C-termini of the peptide were protected by acetyl (Ac) and methyl amide (MA) groups. This accounts for the situation occurring when the (6-13) fragment is embedded in a longer peptide and also avoids undesirable electrostatic interactions, which would occur if the termini were charged.

During the sampling procedure, several interatomic distances of interest were calculated and stored for each selected conformational state. Distances with very small variance are not discriminant and were rejected. Therefore 24 distances were used for multidimensional data analysis: the $m = 24$ measurements (interatomic distances) for the $n = 2735$ objects (conformers) gave a (n*m) data matrix, which was then used in the clustering and partition methods. The most characteristic distances are listed in Table 1 and presented in Fig. 1. These distances are symmetrically distributed in relation to the center of the peptide, such as $C_\alpha(His^6)...C_\alpha(Leu^{10})$ and $C_\alpha(His^9)...C_\alpha(Tyr^{13})$. This presents the further advantage of separately describing the N- and C-moieties of the peptide.

Determination of conformational classes

The principle of all clustering techniques consists in reducing the number of data points by

*The Monte-Carlo procedure acts more or less as a minimizer, while working in the Markovian well-known process; consequently E_{moy} has a rather high value, resulting from a distribution well away from a Gaussian distribution.

TABLE 1
CHARACTERISTIC DISTANCES IN THE PEPTIDE

Distance	Atom 1	Group 1	Atom 2	Group 2
d_1	C_α	(Ac)	C	(His^9)
d_2	C_α	(Ac)	C	(Leu^{10})
d_3	C_α	(Ac)	C	(Leu^{11})
d_4	C_α	(Ac)	C	(Val^{12})
d_5	C_α	(Ac)	C	(Tyr^{13})
d_6	C_α	(His^6)	C	(Leu^{10})
d_7	C_α	(His^6)	C	(Leu^{11})
d_8	C_α	(His^6)	C	(Val^{12})
d_9	C_α	(His^6)	C	(Tyr^{13})
d_{10}	C_α	(His^6)	C	(MA)
d_{11}	C_α	(Pro^7)	C	(Leu^{11})
d_{12}	C_α	(Pro^7)	C	(Val^{12})
d_{13}	C_α	(Pro^7)	C	(Tyr^{13})
d_{14}	C_α	(Pro^7)	C	(MA)
d_{15}	C_α	(Phe^8)	C	(Val^{12})
d_{16}	C_α	(Phe^8)	C	(Tyr^{13})
d_{17}	C_α	(Phe^8)		(MA)
d_{18}	C_α	(His^9)	C	(Tyr^{13})
d_{19}	C_α	(His^9)	C	(MA)
d_{20}	C_α	(Leu^{10})	C	(MA)
d_{21}	N	(His^6)	O	(Tyr^{13})
d_{22}	O	(His^6)	N	(His^9)
d_{23}	N_δ	(His^6)	N_ε	(His^9)
d_{24}	C_δ	(Phe^8)	C_ε	(Tyr^{13})

grouping together neighbouring points. Methods of cluster analysis and their applications have been reviewed by several authors [24–26].

The determination of the optimal number of representative clusters is not a simple problem as no unique answer exists concerning the best partition of the clouds into separate clusters. The number of clusters should be small, but the information on each cluster should be great since it is not possible to obtain the best possible partition of the data by using only one clustering method; both partition and hierarchy methods were applied here. Moreover, various statistical criteria are often necessary to obtain a realistic clustering of the objects into well-separated clouds. The SAS software package [27] uses three of these: the well-known cubic clustering criterion (CCC) [28], the 'pseudo F statistic' pSF [29], and the 'pseudo t^2 statistic' pst^2 [26].

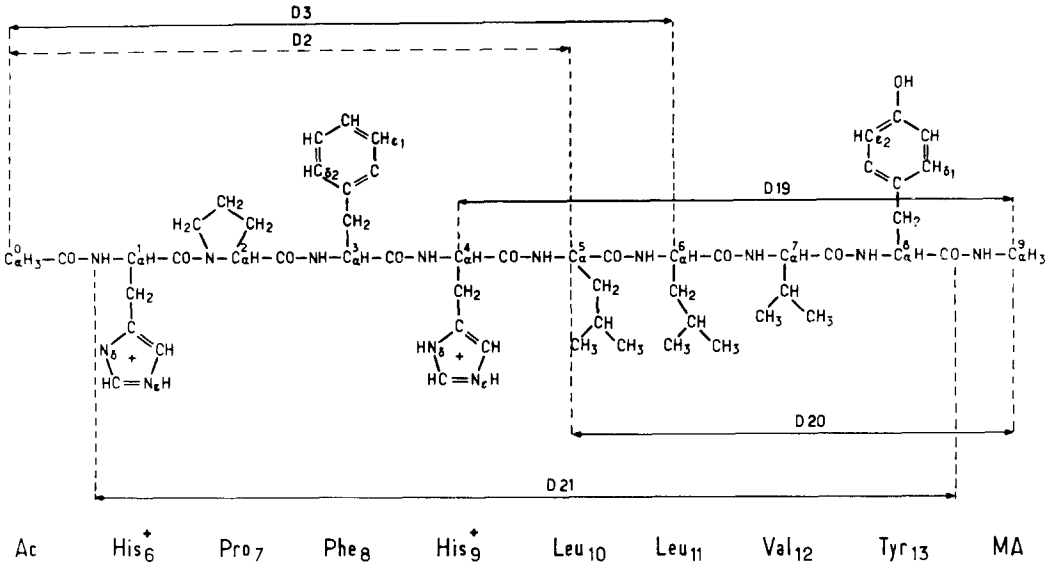

Fig. 1. Representation of the molecule and of a few characteristic distances.

(a) Partition methods

These methods aim at obtaining a sole partition in a predetermined number of classes. The procedure used here is named FASTCLUS and is part of the SAS package; it uses the nearest centroid sorting process [20]. A set of points called cluster seeds is selected as the first guess of the means of the clusters. Each observation is assigned to the nearest seed to form temporary clusters. The seeds are then replaced by the means of the temporary clusters and the process is repeated until no further changes occur in the clusters. FASTCLUS is very efficient for a large data set but requires a precise number of clusters, which is particularly the case for disjoint clusters. FASTCLUS must be run once for each number of clusters.

(b) Hierarchical cluster analysis

There are several possibilities for linking objects together until stable families are obtained, among which are the single, average and complete linkage and the centroid method [25, 26]. The first one is strongly biased to elongated clusters. These techniques are included in the SAS software package.

RESULTS

The use of only hierarchical cluster analysis with the various methods (average and complete linkage and the centroid method) did not allow the determination of a precise number of clusters.

We then successively used the FASTCLUS method and various clustering methods; such a procedure is advised for large data sets with a continuous distribution [25, 26]. This is the case as appeared from a principal component analysis (ACP) of the whole data set.

(1) The data were first partitioned in a reasonably large number of clusters, either 20, 50 or 100 clusters. In the latter case this represents an average of 20–30 observations per cluster. Such reduced clusters may be assumed to be homogeneous.

(2) We then performed various hierarchical cluster procedures (average, complete and centroid methods). The CCC, psF and pst^2 criteria were all in favour of values between 6 and 8 clusters for the lowest number of clusters, and between 10 and 12 for the next highest (see Fig. 2).

(3) The homogeneity of a cluster could be improved by again using the FASTCLUS procedure on the whole data set taking as seeds the cluster means found for each cluster. This allowed a rearrangement of observations between clusters. Figure 2 shows the CCC, pst^2 and psF versus different numbers of clusters, for average linkage used as an example. The presence of peaks is an indication of the optimal number of clusters. This should be a maximum for CCC and psF and a

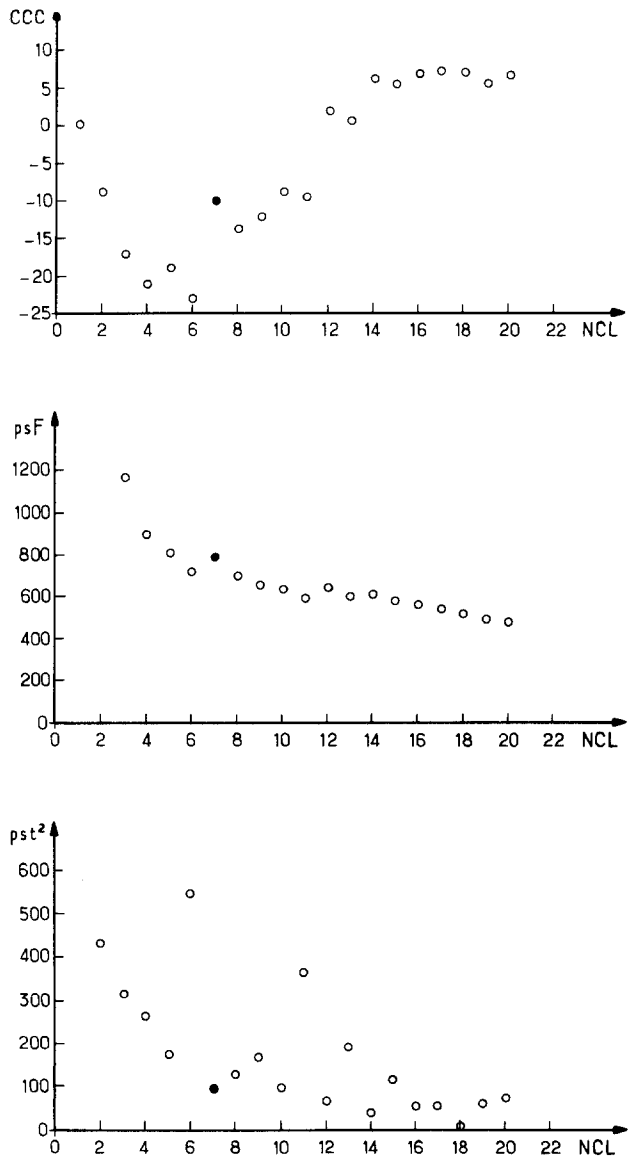

Fig. 2. CCC, psF and pst^2 curves in relation to the number of clusters.

minimum for pst^2. In the present case the most probable numbers of clusters were 7, 10, 12.... The choice between them was arbitrary because information on a 12-cluster distribution was contained in the 7-cluster. The lesser the number of clusters considered the easier is the description of molecular conformation. In the present case, we decided to choose the 7-cluster distribution.

NCL is the retained number of conformers for each cluster; RMSSTD is the root-mean-square standard deviation in Å for each class of conformers, in relation to the 24 interatomic distances:

	CL_1	CL_2	CL_3	CL_4	CL_5	CL_6	CL_7
NCL	209	505	289	153	606	614	359
RMSSTD	1.51	1.53	1.88	2.11	1.72	1.74	1.91

RMSSTD is equal to the root-mean-square distance between observations in the cluster. For a given number of observations in a cluster, the lower the RMSSTD the more homogeneous is the cluster. We can see that clusters 1 and 2 have a similar dispersion, which is significantly lower than those of clusters 5 and 6 and even clusters 4 and 7.

DESCRIPTION OF CLUSTERS

Several significant interatomic distances, as defined in Table 1, with their standard deviations are shown in Table 2, for each cluster and the whole data set. For a given cluster, some distances, d_{21} for instance, differ from the same distances of any cluster and of the whole sample. Small standard deviations correspond to significant distances; for instance most distances of cluster 2 significantly differ from the same distances of the whole data set. We can then describe each class using those significant distances. For instance, in clusters 6 and 7, d_{10}, d_{14}, d_{17}, d_{19} and d_{21} significantly differ; those distances describe the C-terminal part of the peptide. They are all shorter in cluster 7 than in cluster 6. Each cluster can be represented by a conformer, shown in Fig. 3, whose (φ, ψ) angles are shown in Table 3. We do not give the energy of the representative conformation for each cluster, because this latter corresponds to the centroid of each cluster, and not necessarily to the most stable conformer [13]. However, it must be kept in mind that all conformers of a given cluster differ more or less from the representative conformer, which has been represented only to give a rough idea of the shape of conformers belonging to that cluster.

Cluster 1

This cluster has 209 (7.6%) members; conformers have d_2, d_3 and d_4 distances, significantly greater than for the whole set, while d_{17} and d_{19} are significantly lower. These conformers can be described as elongated in the His^6-Pro^7-Phe^8-His^9-Leu^{10} region and folded at Leu^{11} residue level of the C-termini, as can be seen in Fig. 3 for the representative conformer of cluster 1 and (φ, ψ) angles of residues His^6 to Leu^{10}.

Cluster 2

In this cluster with 505 conformers (18.5%), all distances are significantly greater than those of

TABLE 2
MEAN SIGNIFICANT DISTANCES (IN Å) IN EACH CLUSTER

	Population 2735 conf.	CL1 7.6%	CL2 18.5%	CL3 10.6%	CL4 5.6%	CL5 22.4%	CL6 22.4%	CL7 13.1%
D2	12.2	14.8	14.5	8.3	11.4	13.6	10.5	12.0
	(2.7)	(1.0)	(1.5)	(2.5)	(2.0)	(1.5)	(1.8)	(1.9)
D3	13.8	16.9	17.2	8.5	11.4	16.1	11.4	13.1
	(3.4)	(1.5)	(1.7)	(2.2)	(1.8)	(1.8)	(1.7)	(1.8)
D4	15.3	17.2	20.0	9.0	9.9	17.7	13.7	13.7
	(3.9)	(1.3)	(1.8)	(2.0)	(2.0)	(1.6)	(1.7)	(1.7)
D5	16.4	14.9	22.5	10.5	8.2	18.8	15.5	14.4
	(4.4)	(1.7)	(1.7)	(1.9)	(2.1)	(1.5)	(1.7)	(1.6)
D7	11.6	13.8	14.4	7.6	9.3	13.6	9.6	10.9
	(2.8)	(1.1)	(1.5)	(1.6)	(1.4)	(1.5)	(1.3)	(1.9)
D8	13.3	14.4	17.4	8.9	8.5	15.3	12.1	11.6
	(3.2)	(1.3)	(1.5)	(1.6)	(1.2)	(1.4)	(1.2)	(1.8)
D9	14.7	12.2	19.9	10.9	7.6	16.5	14.2	12.4
	(3.7)	(1.8)	(1.4)	(1.5)	(1.3)	(1.3)	(1.5)	(1.4)
D10	16.3	11.0	22.4	13.1	8.1	18.0	16.9	13.0
	(4.3)	(1.0)	(1.7)	(1.9)	(1.8)	(1.7)	(1.5)	(2.0)
D14	15.6	8.6	20.2	15.4	9.2	16.1	17.6	12.1
	(4.0)	(1.2)	(1.6)	(1.9)	(1.9)	(2.1)	(1.7)	(2.0)
D17	14.2	7.2	17.8	15.5	10.2	14.1	15.7	11.2
	(3.4)	(1.6)	(1.4)	(1.6)	(2.3)	(1.8)	(1.6)	(1.8)
D19	12.5	6.9	14.6	14.0	10.7	11.9	14.2	10.2
	(2.9)	(1.5)	(1.3)	(1.8)	(3.1)	(1.9)	(1.5)	(1.6)
D21	16.1	14.7	21.9	11.9	7.6	18.3	16.1	13.2
	(4.2)	(1.0)	(1.6)	(1.7)	(1.7)	(1.6)	(1.5)	(1.9)

Standard deviations in parentheses.

the whole set. It can be described as fully extended with a d_{21} distance as high as 21.9 Å. Side chains are alternately on each side of the main chain as is the case for a β-pleated sheet structure. This can be clearly seen in Fig. 3 and in the (φ, ψ) angles of all residues but His^6.

Cluster 3

On one hand, this cluster with 289 conformers (10.6%) is folded in the Pro^7-Phe^8-His^9 region of the N-terminal moiety, as suggested by the distances from d_2 to d_{10} and (φ, ψ) angles Pro^7, Phe^8.

TABLE 3
(φ, ψ) ANGLES FOR RESIDUES OF EACH CLUSTER (°)

	Cluster 1		Cluster 2		Cluster 3		Cluster 4		Cluster 5		Cluster 6		Cluster 7	
	φ	ψ	φ	ψ	φ	ψ	φ	ψ	φ	ψ	φ	ψ	φ	ψ
His^{6}	−174	154	55	65	−157	66	−151	150	−172	96	−159	89	−162	67
Pro^{7}	−60	89	−60	142	−60	−50	−60	90	−60	165	−60	−50	−60	−40
Phe^{8}	−127	154	−64	123	−174	−61	−176	149	−176	149	−94	178	−75	138
His^{9}	−155	117	−159	88	−151	40	−73	−157	−63	137	−74	−50	−162	162
Leu^{10}	−85	96	−48	147	−12	88	−83	169	−112	154	−180	141	−92	−56
Leu^{11}	56	62	−131	30	−95	83	70	−174	−136	62	−93	106	−90	110
Val^{12}	42	66	−105	129	−98	137	−116	132	113	−55	−88	106	−54	117
Tyr^{13}	−72	173	−72	173	−116	138	−144	166	50	40	−180	132	−67	−50
E_{min}	2.8		0.0		3.5		4.6		2.1		5.1		5.7	
E_{moy}	5.7		3.1		6.2		6.5		4.9		7.3		7.9	

On the other hand, the Leu^{10}-Leu^{11}-Val^{12}-Tyr^{13} moiety represented by d_{17}, d_{19} and d_{21} is rather elongated (on the whole, cluster 3 can be considered to be folded).

Cluster 4

This cluster, with only 153 conformers (5.6%), is rather dispersed with an RMSSTD of 2.11. It is globally folded as attested by several distances (d_2, d_3...d_{21}). This folding is well-illustrated by the representation of the average conformation (Fig. 3) and can be seen in the (φ, ψ) angles of Phe^{8}, His^{9} and Leu^{11}.

Cluster 5

This cluster with 606 conformers (22.2%) is rather elongated as far as the His^{6}-Pro^{7}-Phe^{8}-His^{9}-Leu^{10}-Leu^{11} region is concerned, but slightly less extended than cluster 2, as shown by several distances (d_9, d_{10}...d_{21}). The (φ, ψ) angles of the representative conformer correspond to an elongated peptide for all residues except Leu^{11} and Val^{12}.

Cluster 6

This cluster with 614 conformers (22.4%) can be considered as folded as far as His^{6}-Pro^{7}-Phe^{8}-His^{9} is concerned (distances d_2, d_3, d_7) and extended for the remaining tetrapeptide (distances d_{14}, d_{17} and d_{19}), in good agreement with (φ, ψ) angles.

Cluster 7

This cluster with 359 conformers (13.1%) is as folded as cluster 6 as far as His^{6}-Pro^{7}-Phe^{8}-His^{9} is concerned, according to many distances and (φ, ψ) angles. However, it appears less extended for the C-terminal moiety (distances d_{14}, d_{17}, d_{19}, d_{20}) and (φ, ψ) angles of Leu^{10} and Tyr^{13}.

A thorough examination of the distances in Table 3 shows a great similarity of distances in clusters 2 and 5; they are, however, slightly more elongated for cluster 2 than for cluster 5. However,

c11

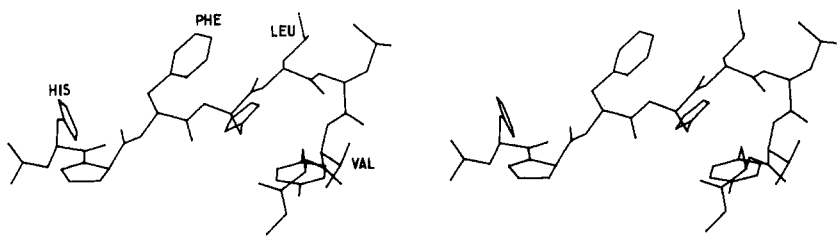

c12

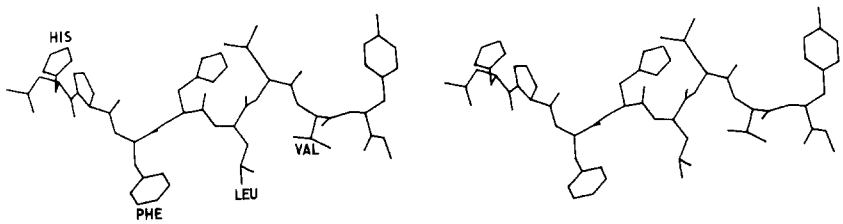

c13

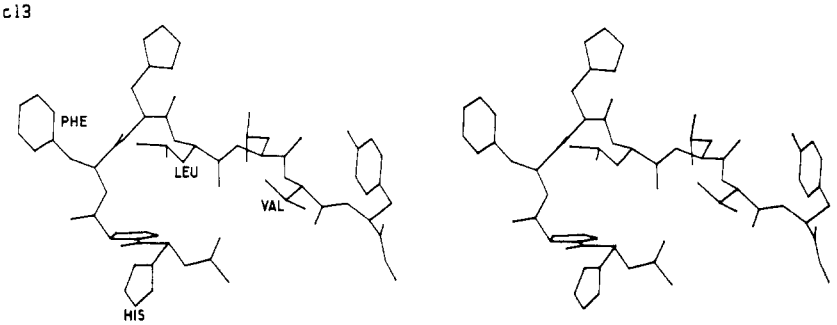

c14

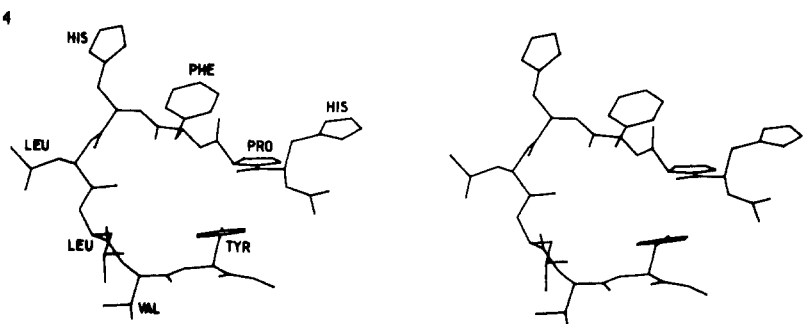

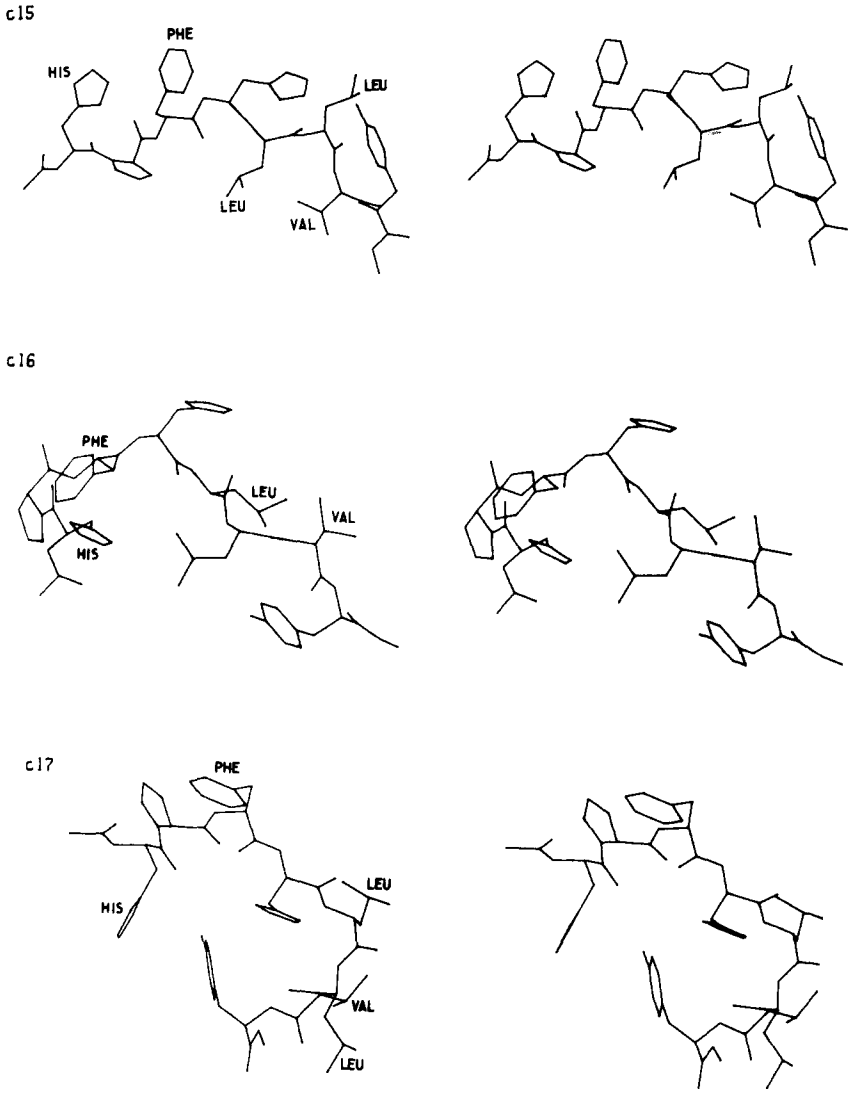

Fig. 3. Characteristic conformers of the seven clusters (CL1: cluster 1, etc.)

clusters 2 and 5 cannot be considered as identical. Their conformation can be considered as extended, making a group of 1111 conformers (40.6% of the distribution).

CONCLUSION

The present study shows the great flexibility of the angiotensinogen (6-13) octapeptide. About 40% of conformers (clusters 2 and 5) can be considered as extended and about 29% (clusters 3, 4 and 7) are rather folded.

Our results can be compared very cautiously with those obtained on other renin inhibitors. The

crystal structure of two complexes between renin inhibitors and peptidases related to renin has been solved:

(1) Pro-His-Pro-Phe-His-Leu-ψ (CH_2NH)-Val-Ile-His-Lys with endothiapepsin [30].

(2) Pro-Phe-His-Phe-ψ (CH_2NH)-Phe-Val with rhizopuspepsin [31].

In both complexes the inhibitors are quite extended with a deformation at the ψ (CH_2NH) level.

It must be emphasized, however, that if there is a similarity between the N-terminal moiety of these inhibitors and angiotensinogen (6-9), their C-terminal moiety has little kinship with angiotensinogen (10-13).

It is worth comparing the conformation proposed by Oliveira et al. [32] for the tetradecapeptide containing the N-terminal sequence of equine renin substrates. This model contains a (9-6) β-turn involving His^6 to His^9, which is stabilized by interactions between the β-antiparallel Val^3-Tyr^4-Ile^5 and Leu^{10}-Leu^{11}-Val^{12} structures and by electrostatic interactions between the N- and C-terminal ends of the molecule. While the N-terminal sequence is missing, similar conformations appear in cluster 3, and folded structures without a β-turn are present in cluster 4.

Although the crystal structure of angiotensinogen (6-13) has not yet been solved, the structures of some of their fragments are somewhat comparable to the conformers in this study.

The crystal structure of Ac-Pro-Phe-His and molecular mechanics calculations on Ac-His-Pro-Phe-His-MA are in favor of a β-turn [9]. In the crystalline state both Leu-Leu-Val-Tyr-OMe [10] and φ-O-CH_2O-Leu-Val-Phe-OMe [11] adopt a β-pleated sheet conformation, in agreement with conformers of clusters 2 and 5.

The conformational flexibility of the angiotensinogen (6-13) fragment is underlined by the fact that the 7 different clusters, although having very different characteristic distances, are endowed with ΔE-relative energy differences characterizing their best individual representatives (mathematically the nearest of the centre of gravity of each cluster). They are, of course, within the 10 kcal/mol interval from one another.

At present experimental results concerning the active angiotensinogen (6-13) are very limited indeed. Information obtained from small fragments should be considered very cautiously.

ACKNOWLEDGEMENTS

We thank Drs. B. Gresh and M. Kreissler for stimulating and helpful discussions.

REFERENCES

1 Skeggs, L.T., Kahn, J.R., Lentz, K.E. and Shumway, N.P., J. Exp. Med., 106 (1957) 439.
2 Tewksburg, D.A., Dart, R.A. and Travis, J., Biochem. Biophys. Res. Commun., 91 (1981) 1311.
3 Matsoukas, J.M. and Moore, G.J., Biochem. Biophys. Res. Commun., 122 (1984) 434 and references therein.
4 Fox, J.W. and Tu, A.T., Arch. Biochem. Biophys., 201 (1980) 375.
5 Marchionini, C., Maigret, B. and Premilat, S., Biochem. Biophys. Res. Commun., 112 (1983) 339.
6 Abillon, E., C.R. Acad. Sci. Paris, Série III, 296 (1983) 893.
7 Nikiforovich, G.V., Vesterman, B., Betins, J. and Podino, L., J. Biomol. Struct. Dyn., 4 (1987) 1119 and references therein.
8 Nakaie, R., Oliveira, C.F. and Juliano, L., Biochem. J., 205 (1982) 43 and references therein.
9 Benkoulouche, M., Cotrait, M., Geoffre, S. and Precigoux, G., Int. J. Pept. Prot. Res., 34 (1989) 463.
10 Precigoux, G., Courseille, C., Geoffre, S. and Leroy, F., J. Am. Chem. Soc., 109 (1987) 7463.
11 Geoffre, S., Leroy, F. and Precigoux, G., Int. J. Pept. Prot. Res., 27 (1986) 454.

12 Metropolis, N.A., Rosenbluth, A.W., Teller, A.H. and Teller, E.J., J. Chem. Phys., 21 (1953) 1087.
13 Kreissler, M., Pesquer, M., Maigret, B., Fournie-Zaluski, M.C. and Roques, B.P., J. Comput.-Aided Mol. Design, 3 (1989) 85.
14 Cotrait, M., Kreissler, M., Lehn, J.-M. and Maigret, B., J. Comput.-Aided Mol. Design, (1991) in press.
15 Li, Z. and Scheraga, H., Proc. Natl. Acad. Sci. U.S.A., 84 (1987) 6611.
16 Premilat, S. and Maigret, B., J. Phys. Chem., 84 (1980) 293.
17 Maigret, B. and Premilat, S., Biochem. Biophys. Res. Commun., 104 (1982) 971.
18 Premilat, S. and Maigret, B., Biochem. Biophys. Res. Commun., 91 (1979) 534.
19 Janin, J., Wodak, S., Levitt, S. and Maigret, B., J. Mol. Biol., 125 (1978) 357.
20 Lowry, G.C. (Ed.), Markov Chain and Monte-Carlo Calculations in Polymer Science, Marcel Dekker, New York, 1970.
21 Scheraga, H.A., Adv. Phys. Org. Chem., 6 (1968) 103.
22 Cotrait, M., Int. J. Pept. Prot. Res., 22 (1983) 110.
23 Cotrait, M. and Ptak, M., J. Comput. Chem., 2 (1981) 460.
24 Milligan, G.W., Psychometrika, 45 (1980) 325.
25 Duran, B.S. and Odell, P.L., Cluster Analysis: A Survey (Lecture Notes in Economics and Mathematical Systems), Springer-Verlag, New York, 1974.
26 Duda, R.O. and Hart, P.E., Pattern Classification and Scene Analysis, Wiley, New York, 1983.
27 SAS Institute Inc., Box 8000, Cary, NC 27511, U.S.A.
28 Sarle, W.S., SAS Technical Report A-108 (1983), SAS Institute Inc., NC 27511, U.S.A.
29 Calinski, T. and Harabasz, J., Comm. Statistics, 3 (1974) 1.
30 Suguma, K., Padlan, E.A., Smith, C.W., Carlson, W.D. and Davies, D.R., Proc. Natl. Acad. Sci. U.S.A., 84 (1987) 7009.
31 Foundling, S.I., Cooper, J., Watson, F.E., Cleasby, A., Pearl, L.H., Sibanda, B.L., Hemmings, A., Woods, S.P., Blundell, J.L., Valler, M.J., Norey, C.G., Kay, J., Boger, J., Dunn, B.M., Leckie, B.J., Jones, D.M., Atrash, B., Hallett, A. and Szelke, M., Nature 327 (1987) 349.
32 Oliveira, M.C.F., Juliano, L.L. and Paiva, A.C.M., Biochemistry, 16 (1977) 2606.